Ecological Engineering 156 (2020) 105973

Contents lists available at ScienceDirect

Ecological Engineering

journal homepage: www.elsevier.com/locate/ecoleng

Quantifying the impacts of lithology on vegetation restoration using a random forest model in a karst trough valley, China

Yina Qiao[a], Hui Chen[b], Yongjun Jiang[a,*]

[a] Chongqing Key Laboratory of Karst Environment & School of Geographical Sciences, Southwest University, Chongqing 400715, China
[b] School of Resources and Environment, University of Electronic Science and Technology of China, Chengdu 611731, China

ARTICLE INFO

Keywords:
NDVI
Lithology
Random forest
Karst trough valley

ABSTRACT

Karst regions in southwest China are characterized by vulnerable ecological environment. Knowledge on the driving factors of vegetation cover change could provide valuable information for ecological restoration management. However, quantitative identification of the key drivers for the vegetation restoration remains challenging in karst trough valleys. In this study, we used normalized difference vegetation index (NDVI) time series (2000–2016), Theil-Sen median analysis, Mann-Kendall trend test, and Hurst exponent to analyze the vegetation cover trends in a karst trough valley. The performance of multiple linear regression (MLR), generalized additive models (GAM), support vector machine (SVM), and random forest (RF) in accounting for vegetation cover change were compared. The results showed that vegetation cover trends for increasing, stable and decreasing accounted for 71.44%, 28.16% and 0.40% of the study area, respectively. Lithology had a significant effect on spatial patterns of temporal change and future sustainability in NDVI ($p < .01$). RF performed much better than MLR, GAM and SVM in accounting for vegetation cover change. The RF model had much lower fitting error indices (MAE = $1.46*10^{-3}$, RMSE = $1.92*10^{-3}$) and higher R^2 (0.65) than MLR, GAM and SVM models. Thus, RF model was applied to identify impacts of driving factors on vegetation cover change quantitatively. Precipitation change, lithology and elevation were key factors for vegetation cover change. The vegetation restoration and reconstruction projects should pay more attention to the region where limestone and above-900 m elevation dominate, due to relatively slow vegetation growth in these regions. The new understandings obtained in this study enrich our knowledge of the effects of lithology and topography on the vegetation cover change and are necessary to guide sustainable projects of ecological recovery in karst trough valleys.

1. Introduction

Southwestern karst regions of China are typical ecologically fragile areas. The largest contiguous exposed carbonate rocks in the world are distributed in southwest China (Jiang et al., 2014). The hard carbonate rocks, which are mainly deposited before the Triassic period, and abundant precipitation in summer lead to developed karst process in southwest China (Yuan, 1997; Wang et al., 2004a, 2004b). Intense chemical dissolution of carbonate rocks forms an underground hydrological structures, which result in rapid percolation of rainfall into the underground (Zhou et al., 2012). The low rate of soil formation and most karst soil lacking a C horizon make it contact with bedrock directly and be susceptible to erosion under intense precipitation (Cao et al., 2004). In the past decades, the ecological deterioration of the karst regions in southwest China is faced with destruction of vegetation, soil erosion, and even rocky desertification (Jiang et al., 2014; Wang et al., 2019). The heavy soil erosion and the loss of water through underground conduits in karst regions result in the poor crop production. Furthermore, eroded soils often fill up the conduits and drainage outlets in karst lowlands, which bring about waterlogging in arable lands. Karst rocky desertification has been the most severe ecological issue exacerbating the poverty of the southwest China (Yuan, 1997; Shao et al., 2006). A series of ecological restoration projects have been implemented by local government to restore and rebuild vegetation in order to combat karst rocky desertification and promote sustainable development.

Vegetation cover change have been recognized as a primary importance index of the stability of terrestrial ecosystems (Jiang et al., 2017; Gang et al., 2018). Normalized Difference Vegetation Index (NDVI), a proxy for photosynthetically active vegetation, is strongly

* Corresponding author at: Chongqing Key Laboratory of Karst Environment & School of Geographical Sciences, Southwest University, Beibei, Chongqing 400716, China.
E-mail address: jiangjyj@swu.edu.cn (Y. Jiang).

https://doi.org/10.1016/j.ecoleng.2020.105973
Received 14 April 2020; Received in revised form 8 July 2020; Accepted 11 July 2020

correlated with percentage vegetation cover. The value of NDVI has been widely used to represent vegetation cover at regional and global scales (Chang et al., 2016; Kang et al., 2017; Zewdie et al., 2017; Szilárd et al., 2018). A global greening trend has been observed in vegetation in recent decades using NDVI time series (Liu et al., 2015). Numerous studies have showed a general increasing trend of vegetation cover in karst regions of southwest China during past two decades (Cai et al., 2014; Tong et al., 2017). Knowledge on the mechanism by which vegetation cover change contributes to protection and restoration of fragile ecological environments. Therefore, the increasing number of studies focused on revealing driving factors for vegetation cover change (Jiang et al., 2017; Pan et al., 2017; Qi et al., 2019). Precipitation has been considered the most important factor influencing vegetation growth in the semi-arid regions (Fensholt et al., 2012), while temperature is a limiting factor for the vegetation cover change in high-latitude areas (Tucker et al., 2001). Recent studies have revealed that changes in land use type induced by human activities were found to be primary factors influencing vegetation growth (Zhao et al., 2017; Chen et al., 2019). The effects of climate (Zhou et al., 2018; Liu et al., 2018), topography (Tong et al., 2016) and ecological engineering projects (Zhang et al., 2018; Tong et al., 2019) on vegetation growth have been proved in karst regions. However, fragile karst ecological environment mainly results from the characteristics of carbonate rocks. Lithology dominates the spatial heterogeneity of the ecological environment in karst regions (Wang et al., 2004b; Jiang et al., 2014). Characteristic of lithology should be considered in the ecological restoration measures instead of copying successful experience in other regions. However, the spatial heterogeneity of vegetation cover change caused by lithology and the impacts of lithology to vegetation cover change in karst regions have not yet been explored. Another problem with previous researches is that the methods of identifying the driving factors for vegetation cover change assume that these relationships are linear. Linear regression, correlation analysis, and residual analysis have been the most commonly used method, the preference of these linear methods result from their simplicity and straightforward interpretation (Cai et al., 2014; Jiang et al., 2017; Qi et al., 2019). In fact, these relationships are complex (Gao et al., 2012; Peng et al., 2019b). It is, therefore, necessary to choose an appropriate method to understand the driving factors of vegetation cover change under a nonlinear and nonstationary assumption. Nonlinear regression and machine learning methods have been applied to account for the complex relationship in many fields, such as economic (Chatzis et al., 2018; Basak et al., 2019), medicine (Steyrl et al., 2015), biology (Fukuda et al., 2014) and agriculture (Guo et al., 2015), but not yet in the research on vegetation cover change.

Therefore, the objectives of this study are to (1) analyze spatial heterogeneity of vegetation cover change and (2) quantify the impacts of driving factors on vegetation cover change using an appropriate model in a karst trough valley of southwestern China.

2. Materials and methods

2.1. Study area

The study area (108°43′08″-109°08′08″E and 28°21′49″-29°24′25″N) is located in Youyang county, southeast of Chongqing, China (Fig. 1). The study area covers 1710 km^2, and approximately 1320 km^2 are karst regions, which are underlain by homogenous dolomite (51.76%), homogenous limestone (18.15%) and impure carbonate rocks (30.09%) (Fig. 2a). The topography is trough valley with elevation ranging from 272 m to 1602 m. The average elevations of the regions underlain by homogenous dolomite, homogenous limestone, impure carbonate rocks and non-carbonate rocks are 734 m, 974 m, 810 m and 678 m, respectively. The climate is subtropical humid monsoon with a mean annual temperature of 17.1 °C and a mean annual precipitation of 1100 mm. Rainfall occurs mainly between April and August. The land-use types are forestland (46.41%), grassland (30.24%), urban-rural land (0.41%), and cultivated land (22.94%) (Fig. 2b). To protect and improve the ecological environment in karst regions of southwestern China, the National Reform and Development Commission of China commenced implementation of a pilot karst rocky desertification restoration project for in the karst regions. Youyang County is one of pilot areas in 2008.

2.2. Data and processing

The MODIS NDVI dataset from 2000 to 2016 with a temporal resolution of 16 days and spatial resolution of 250 m was used in this study. The dataset was collected from LAADS DAAC (https://ladsweb.modaps.eosdis.nasa.gov/), which have been corrected by radiation, geometry and atmosphere. The maximum value composite (MVC) method was used to obtain the monthly NDVI and further composite annual maximum NDVI, which represented the most vigorous condition during a single year. Vegetation cover change was analyzed using annual maximum NDVI in this study. The land-use type dataset was MODIS MCD12Q1 land use/cover at a 500 m spatial resolution.

Annual average temperature and annual precipitation spatial interpolation datasets at 1 km were derived from Resource and Environment Data Cloud Platform (http://www.resdc.cn/). They were further applied to calculate the average annual temperature and precipitation (TEMmean and PREmean), and temporal changes (TEMslope and PREslope) from 2000 to 2016. The spatial distribution of carbonate rocks in study area was extracted from hydrogeological map at a scale of 1:50000. A digital elevation model was downloaded from the US Geological Survey Earth Resources Observation Systems data center, with a spatial resolution of 30 m. Six topographic variables, namely, elevation (Elevation, m), slope (Slope, °), Surface Curvature Index (Cs), relief (Relief, m), Topographic Position Index (TPI) and Topographic Wetness Index (TWI) were calculated from the DEM (Table 1). All topographic variables were calculated by SimDTA1.0.3 software (Qin et al., 2009).

2.3. Method

2.3.1. Temporal trends analysis

Theil-Sen median (TS) trend analysis (Sen, 1968) combined with the Mann-Kendall (M-K) test (Mann, 1945) were applied to analyze the temporal change of NDVI. The advantages of this method are that it does not require data obeying a certain distribution, and has a strong resistance to data errors. The TS formula is:

$$\beta_{NDVI} = M\text{edian}\left(\frac{NDVI_j - NDVI_i}{j - i}\right) \quad 2000 \le i < j \le 2016 \tag{1}$$

when $\beta_{NDVI} > 0$, the NDVI presents an uptrend, otherwise NDVI presents a downtrend.

Mann-Kendall is a non-parametric statistical test method used to determine the significance of NDVI trends.

For $NDVI_j$ time series,

$$Z = \begin{cases} \dfrac{S-1}{\sqrt{V\text{ar}(s)}} & S > 0 \\ 0 & S = 0 \\ \dfrac{S+1}{\sqrt{Var(s)}} & S < 0 \end{cases} \tag{2}$$

where

$$V\text{ar}(s) = \frac{n(n-1)(2n+5)}{18} \tag{3}$$

$$S = \sum_{i=1}^{n-1} \sum_{j=i+1}^{n} \text{sgn}(NDVI_j - NDVI_i) \tag{4}$$

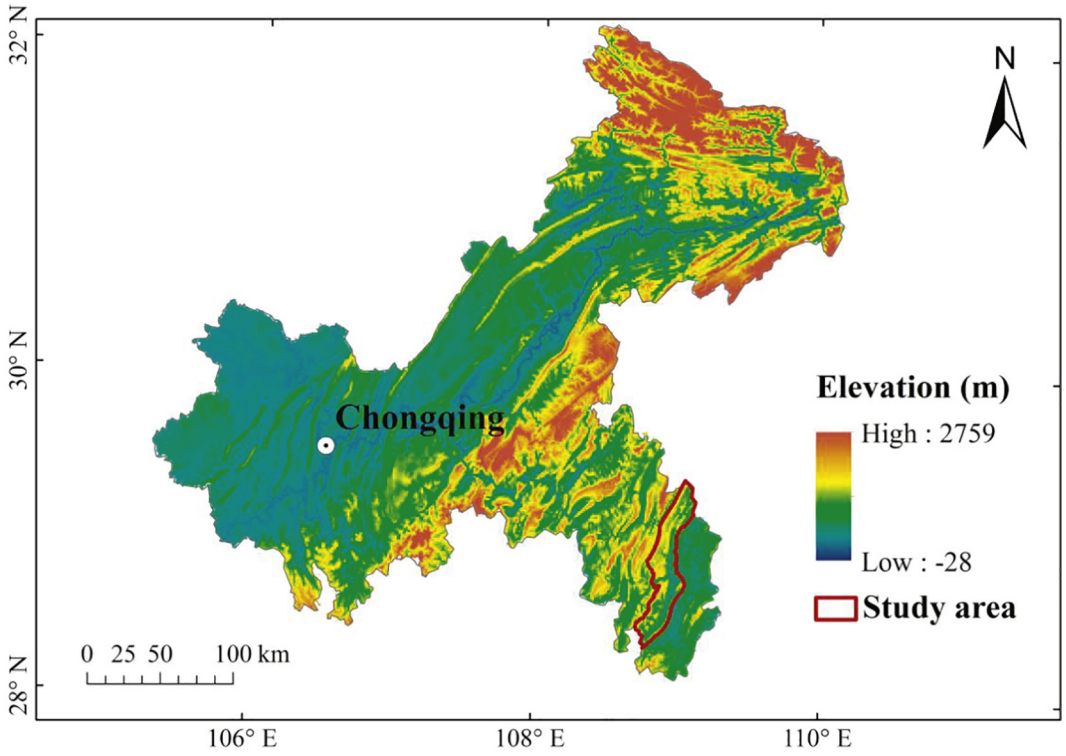

Fig. 1. Location of the study area.

$$\mathrm{sgn}(NDVI_j - NDVI_i) = \begin{cases} 1, & NDVI_j - NDVI_i > 0 \\ 0, & NDVI_j - NDVI_i = 0 \\ -1, & NDVI_j - NDVI_i < 0 \end{cases} \quad (5)$$

where $NDVI_j$ and $NDVI_i$ represent the NDVI values in years i and j, respectively, and n represents length of the time series. If $|Z| > 1.96$, it indicates a significant change in the NDVI time series at the 0.05 level. Thus, the vegetation cover trends were categorized as three types: increasing ($\beta_{NDVI} > 0$ and $|Z| > 1.96$), decreasing ($\beta_{NDVI} < 0$ and $|Z| > 1.96$) and stable ($-1.96 \leq Z \leq 1.96$).

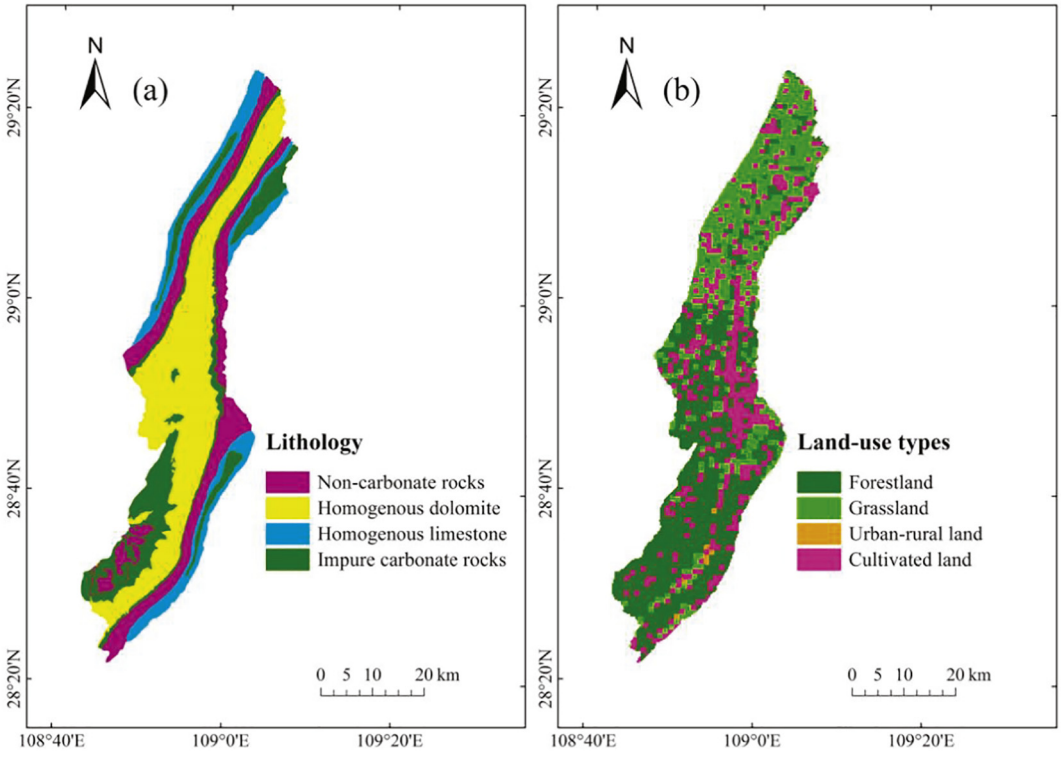

Fig. 2. The spatial patterns of lithology (a) and land-use types (b) of the study area.

Table 1
Definition of selected topographic variables.

Topographic variables	Units	Definition
Elevation	m	The height of a location above sea level
Slope	Degree	The steep degree of a surface topographical point
Relief	m	The differences between the elevation value of the highest topographical point and those of the lowest location within a specific area.
Surface curvature index (Cs)	Dimensionless	An index indicate the curvature of three-dimensional surface landform and magnitude of slope gradient.
Topographic position index (TPI)	Dimensionless	The difference between the elevation value of a position and the average elevation of the neighborhood around that position.
Topographic wetness index (TWI)	Dimensionless	An index indicate the spatial distribution of soil moisture and surface saturation

2.3.2. Future trends analysis

The rescaled range (R/S) analysis is an effective way to quantitatively describe the long-term dependence of time series (Hurst, 1951). The principle of R/S is as follow:

A NDVI time series$\langle NDVI\rangle_\tau$ is defined as:

$$\langle NDVI\rangle_\tau = \frac{1}{\tau}\sum_{t=1}^{\tau} NDVI_{(t)} \quad \tau = 1,\ 2,\ \ldots,\ n \tag{6}$$

The accumulated deviation is calculated as:

$$X_{(t,\ \tau)} = \sum_{t=1}^{\tau} (NDVI_{(t)} - \langle NDVI\rangle_\tau) \quad 1 \le t \le \tau \tag{7}$$

The range sequence is calculated as:

$$R_{(\tau)} = \max_{1\le t\le\tau} X_{(t,\ \tau)} - \min_{1\le t\le\tau} X_{(t,\ \tau)} \quad \tau = 1,\ 2,\ \ldots,\ n \tag{8}$$

The standard deviation sequence is calculated as:

$$S_{(\tau)} = \left[\frac{1}{\tau}\sum_{t=1}^{\tau}\left(NDVI_{(t)} - \langle NDVI\rangle_\tau{}^2\right]^{\frac{1}{2}} \quad \tau = 1,\ 2,\ \ldots,\ n \tag{9}$$

where n represents length of the NDVI time series.

Assume that:

$$\frac{R_{(\tau)}}{S_{(\tau)}} \propto \tau^H \tag{10}$$

H value is called the Hurst exponent. When $0.5 < H < 1$, NDVI time series is a continuous sequence, that means the future vegetation cover trends are consistent with the trend of the past. When $0 < H < 0.5$, NDVI time series has the anti-persistence, that is, the future vegetation cover trends are contrary to the trends of the past. The future trends in vegetation cover were classified into six categories according to the H value and the temporal change determined by TS and M-K test in NDVI (Table 2). When H value was higher than 0.5, and the pixel showed an increasing trend of vegetation cover, the vegetation cover in this pixel is likely to continue to experience an increasing trend (Sustainable increasing) in the future. If the trend was decreasing and its H value was higher than 0.5, the vegetation cover in this pixel is likely to continue to show a decreasing trend (Sustainable decreasing) in the future. When a pixel was detected to have no significant trend (Stable) and its H value was higher than 0.5, the vegetation in this pixel is supposed to have a stable trend (Sustainable stable) in the future. When H value was less than 0.5, and this pixel showed an increasing trend of vegetation cover, the vegetation cover in this pixel is not likely to continue to experience an increasing trend (Anti-sustainable decreasing). If the trend was decreasing but its H value was less than 0.5, the vegetation cover in this pixel is not likely to continue to show a decreasing trend (Anti-sustainable decreasing). If the H value was less than 0.5, and the vegetation cover trend in this pixel was stable, which means the trend is anti-sustainable stable.

Table 2
Future vegetation cover trends based on temporal changes and the H value in NDVI.

Hurst trends	$0 < H < 0.5$	$0.5 < H < 1$
Increasing	Anti-sustainable increasing	Sustainable increasing
Stable	Anti-sustainable stable	Sustainable stable
Decreasing	Anti-sustainable decreasing	Sustainable decreasing

Analysis of variance (ANOVA) was employed to investigate the difference in NDVI values in each region.

2.3.3. Driving factors analysis

Four modeling approaches were employed to fit vegetation cover change. They were multiple linear regression (MLR), generalized additive models (GAM), support vector machine (SVM), and random forest (RF). MLR is a regression model based on classical least square algorithm and assume the relationships between dependent and independent variables are linear. GAM is a non-linear function regression, it could account for non-monotonic relationships in the data (Lin and Zhang, 1999). The response variable is modeled using a Gaussian family with identity link, continuous driving factors were used as non-linear smoothed terms, while categorical driving factors were entered as linear term. GAM was calculated in R using the "mgcv" package. SVM is a supervised machine learning algorithm, which use kernel functions to enlarge the feature space and carry out the nonlinear boundaries by mapping the input vectors into the high-dimensional feature space (Gunn, 1998). SVM was modeled in R using the "rpart" package. RF is developed from decision trees, which combine many decision trees built using bootstrap sampling and choosing randomly at each node a subset of explanatory variables (Breiman, 2001). Three parameters, including number of trees to be grown (n_{tree}), number of variables sampled at each split (m_{try}), and the minimum size of the leaf (*nodesize*) were set to 1000, 5 and 5 respectively. RF was fit in R using the "randomForest" package.

In the four models, the response variable was temporal change of NDVI in each pixel (β_{NDVI}), and the independent variables were the climate variables (TEMmean, PREmean, TEMslope and PREslope), topographic variables (Elevation, Slope, Cs, Relief, TPI and TWI), lithology (non-carbonate rocks, homogenous dolomite, homogenous limestone and impure carbonate rocks) and land-use types (forestland, grassland, urban-rural land and cultivated land) extracted from the corresponding pixel. The *factor* function in R studio was used to define the categorical variables (lithology and land-use types), and it would enter into the models as a binary variable (0 for absence and 1 for presence) for calculation.

In order to assess model performances, 30% pixels were randomly selected from the study area to provide an independent validation dataset, and 70% pixels were used to train models. Coefficient of determination (R^2), mean absolute error (MAE), and root mean square error (RMSE) were calculated to assess the accuracies of the fitted models. The higher accuracy of model, the stronger explanatory power of the driving factors in the model to the change of vegetation cover. The model with the highest accuracy was applied to explore relationships between vegetation cover change and driving factors and to further identify the driving factors on vegetation cover change.

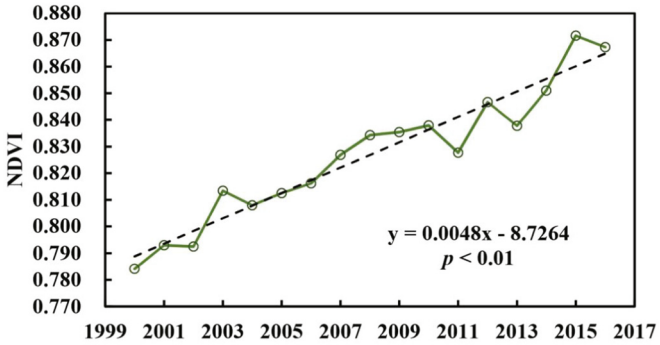

Fig. 3. Inter-annual variation of the NDVI from 2000 to 2016.

3. Results

3.1. Temporal trends of vegetation cover

At regional scale, the NDVI increased significantly at the rate of 0.0048/year ($p < .01$) during 2000–2016 (Fig. 3).

An uptrend in NDVI accounted for 96.51% of the karst trough valley, with 74.02% showing a significant increase. Only 3.49% of the areas showed a downtrend in NDVI, of which 11.55% decreased significantly. Overall, vegetation cover trends of increasing, stable and decreasing accounted for 71.44%, 28.16% and 0.40%, respectively (Fig. 4). The vegetation cover trends at the bottom of the karst trough valley were mainly decreasing and stable, where the homogenous dolomite and cultivated land were dominant.

Lithology and land-use types showed a significant impact on the change rate of NDVI ($p < .01$). The highest rate of increase on NDVI was observed in non-karst region (0.0052/year), followed by the regions underlain by impure carbonate rocks (0.0048/year) and homogenous dolomite (0.0047/year), the lowest rate of increase was observed in homogenous limestone region (0.0044/year). The area percentage of vegetation cover trends in each lithology were shown in Table 3. Relative small percentage area of homogenous limestone region showed an increasing trend in vegetation cover. The increase rate of NDVI for the different land-use types ranked from high to low are forestland (0.0050/year) > grassland (0.0048/year) > cultivated land (0.0043/year) > urban-rural land (0.0034/year). The smallest percentage of increasing trend was observed in the urban-rural land (Table 3).

Table 3
Proportion of vegetation cover trends for different regions.

Regions	Increasing	Stable	Decreasing
Non-carbonate rock	76.33	23.67	0.00
Homogenous dolomite	70.59	28.40	1.01
Homogenous limestone	65.16	34.84	0.00
Impure carbonate rocks	71.82	28.18	0.00
Forestland	76.23	23.69	0.08
Grassland	70.46	29.39	0.15
Urban-rural land	53.15	44.14	2.71
Cultivated land	63.47	35.18	1.35

3.2. Future trends of vegetation cover

Fig. 5a shows the spatial patterns of the H values for the NDVI time-series. The mean H value of the study area was 0.77 ranging between 0.32 and 0.98. The H values in about 98.15% of the study area were greater than 0.5, it indicated that NDVI time-series had a strong positive sustainability. Lithology and land-use types showed a significant impact on H value ($p < .01$). Higher H values were observed in the regions underlain by non-carbonate rocks (0.79) and homogenous dolomite (0.78), followed by impure carbonate rocks (0.77), the lowest H values were occurred in the homogenous limestone (0.75) region. The average H value in each land-use type ranked from high to low was forestland (0.79) > grassland (0.77) > cultivated land (0.76) > urban-rural land (0.74).

Temporal change and the H value in NDVI were combined into 6

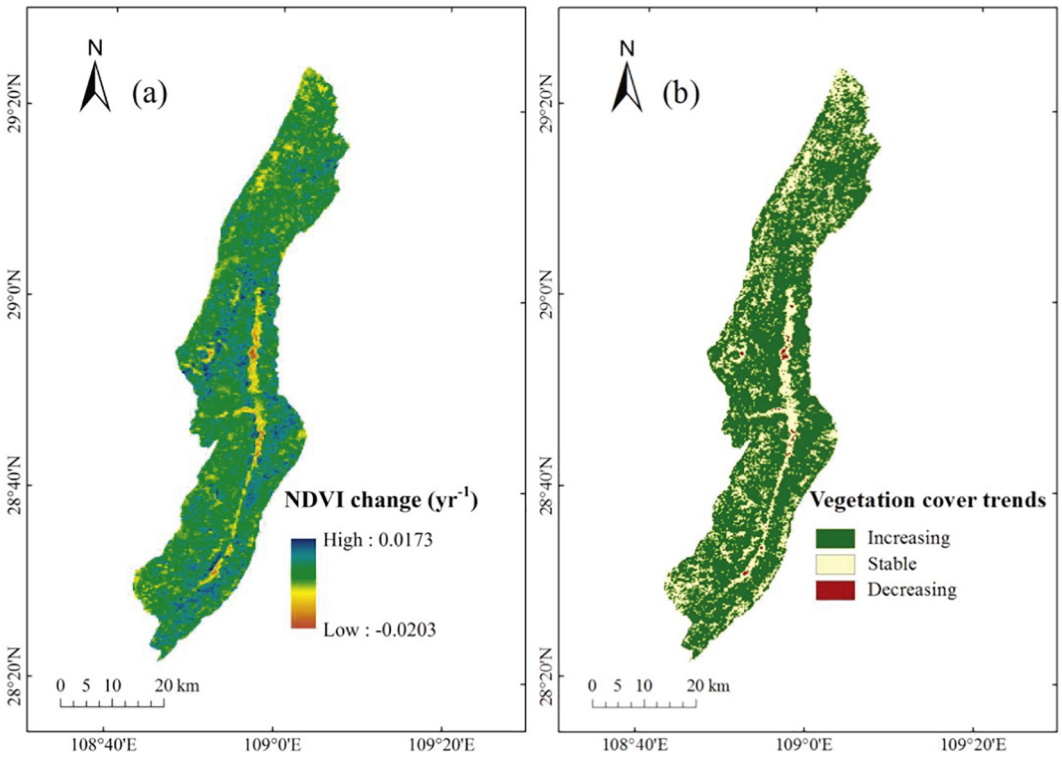

Fig. 4. Spatial patterns of NDVI change and vegetation cover trends from 2000 to 2016.

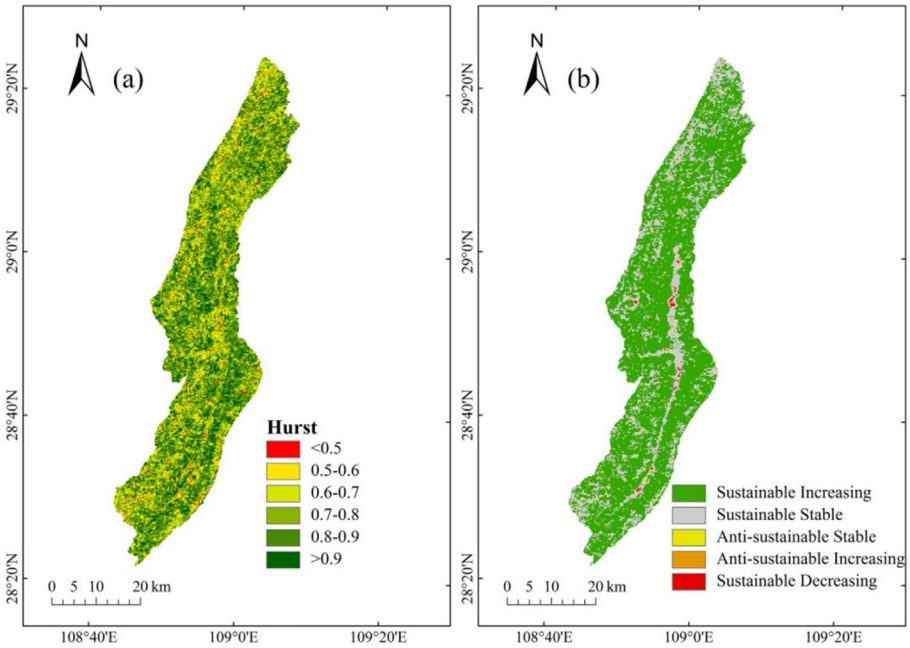

Fig. 5. Spatial patterns in Hurst exponent from 2000 to 2016 (a) and future vegetation cover trends (b).

Table 4
Proportion of future vegetation cover trends in different regions.

Regions	Sustainable increasing	Sustainable stable	Anti-sustainable stable	Anti-sustainable increasing	Sustainable decreasing
Non-karst	76.22	22.09	1.58	0.11	0.00
Homogenous dolomite	70.55	26.77	1.63	0.05	1.00
Homogenous limestone	65.13	32.84	2.00	0.03	0.00
Impure carbonate rocks	71.70	26.15	2.04	0.11	0.00
Forestland	76.15	22.25	1.45	0.07	0.08
Grassland	70.36	27.70	1.70	0.09	0.15
Urban-rural land	53.15	38.74	5.41	0.00	2.70
Cultivated land	63.45	32.74	2.44	0.03	1.34

classes to indicate future vegetation cover trends (Table 2). The *H* values of each pixel where NDVI showed decreasing trend were larger than 0.5, which indicated that the areas with degraded vegetation did not turn better in the future, thus there were five future trends of vegetation cover in the study area (Fig. 5b). Vegetation cover in most of the study area (71.4%) showed a sustainable increasing trend. The lowest share of sustainable increasing vegetation cover trend was found in homogenous limestone and urban-rural land regions (Table 4).

3.3. Driving factors of vegetation cover change

Table 5 presents the fitting error indices derived from validation of the temporal change of NDVI using independent validation dataset. The RF model produced the highest R^2 (R^2 = 0.65), the lowest MAE (MAE = $1.46*10^{-3}$) and RMSE (RMSE = $1.92*10^{-3}$) for temporal change in NDVI value (β_{NDVI}). Therefore, RF was applied to identify the importance of driving factors for vegetation cover change, and further explore relationships between vegetation cover change and main driving factors (Fig. 7) (Fig. 8).

Table 5
Performance comparisons of the MLR, GAM, SVM and RF models.

Models	R^2	MAE	RMSE
MLR	0.33	$1.77*10^{-3}$	$2.36*10^{-3}$
GAM	0.45	$1.70*10^{-3}$	$2.23*10^{-3}$
SVM	0.52	$1.61*10^{-3}$	$2.14*10^{-3}$
RF	0.65	$1.46*10^{-3}$	$1.92*10^{-3}$

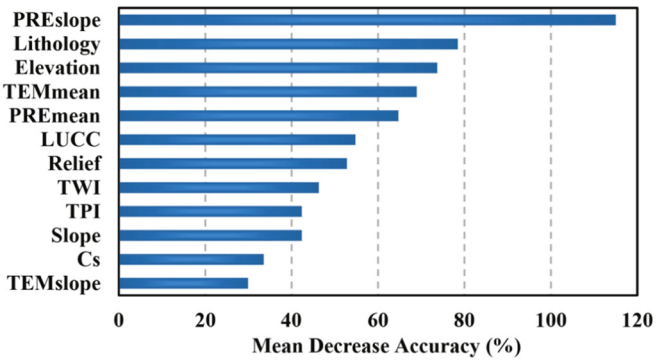

Fig. 6. Relative importance of driving factors for vegetation cover change (LUCC: land-use types; TEMslope: temperature change; TEMmean: average annual temperature; PREmean: average annual precipitation; PREslope: precipitation change).

The mean decrease in mean squared error (MDA) of $\beta_{NDVI}$was used to identify the importance of drivers to vegetation cover change, and the higher the value, the more important it is (Fig. 6). The precipitation change has the highest MDA value, which indicated it was the most important factor for vegetation cover change. Lithology, elevation, average annual temperature and precipitation was the second group of important driving factors, their MDA values were between 60 and 80%. The MDA values of land-use types and four topographic index (Relief,

TWI, TPI and Slope) were between 40 and 60%, they were the third group of driving factors. Cs and temperature change had the weakest impacts on vegetation cover change. In general, climate, lithology, elevation and land-use types were the major driving factors to vegetation cover change.

4. Discussion

4.1. Impacts of lithology on vegetation cover change

Both the analysis of ANOVA and RF model in this study demonstrated lithology contributes to the spatial heterogeneity for vegetation cover change. Acid-insoluble components are low in pure carbonate rocks, which indicate the rate of soil formation is extremely slow due to low amounts of residues left after dissolution (Yuan, 2014). Previous study suggested it would take about 8000 years to form about 1 cm thickness of soil under the present climate (Yuan, 1997; Wang et al., 1999). Soil is pivotal to vegetation growth by nutrient and organic matter supplies, therefore, the lower vegetation cover increases were observed in karst regions than in non-karst region. The differences in lithology between limestone and dolomite determine the modes of dissolution, and result in the spatial heterogeneity of water and soil resources in karst regions (Jiang et al., 2014). The limestone is dominated by differential dissolution, the developed fractures and joints are the places where dissolution mainly occurs. These characteristics of limestone result in the high spatial heterogeneity of topographic features in small-scale, while surface soil lose to underground fractures and conduits. As a result, limestone region is more prone to rocky desertification. Homogeneous dissolution of dolomite results in the relatively uniform and thick distribution of soil and water resources in the dolomite region compared with the limestone region (Wang et al., 1999; Wang et al., 2004b), therefore increasing trend in vegetation cover was pronounced in dolomite region.

4.2. Impacts of climate on vegetation cover change

Precipitation change, the most important factors, showed a stronger effect than temperature to vegetation growth in the study area. This finding is different to previous studies which have suggested that slight changes in precipitation will not affect vegetation growth due to abundant precipitation and moderate temperature in humid and semi-humid areas, temperature is the dominant climate factor effecting vegetation growth (Hou et al., 2015; Lamchin et al., 2017). However, the developed underground hydrological structures and the shallow soil profile result in rapid rainfall infiltration in karst regions (Zhou et al., 2012; Zhou et al., 2018), although the average annual precipitation is 1100 mm in the study area, underground loss of rainfall leads to the strong dependency between vegetation growth and precipitation change. The positive effect between known NDVI and precipitation means that precipitation promote vegetation growth. This is confirmed by the RF modeling, which yields the largest marginal increases on NDVI within the increasing precipitation (Fig. 7a). However, the region with high annual precipitation showed a low marginal NDVI increase (Fig. 7b), this relationship may be due to relative high annual precipitation was occurred in high elevation regions, where limestone dominates in the study area, these regions are sensitive to soil erosion under intense precipitation and not conductive to vegetation growth. Increasing temperature promotes photosynthesis of vegetation and further improves vegetation cover (Fig. 7d), while temperature variation above the favorable temperature of vegetation will accelerate evaporation, which no longer further promote vegetation growth (Fig. 7c).

4.3. Impacts of elevation on vegetation cover change

Topography imposes environmental constraints on vegetation growth (Tao et al., 2017). Previous studies have investigated the impacts of topography on vegetation growth in karst regions (Tong et al., 2016), however, they were not able to quantify the specific advantageous intervals for vegetation restoration. Elevation was identified as the third driving factor and the most important topographic factor for vegetation cover change in our study. Fig. 8 shows the relationship between NDVI temporal change and elevation is not monotonically increasing. The lowest marginal increase rate in NDVI occurred in the lower elevation area (< 500 m). This result may be explained by the fact that the regions dominated by lower elevation are more suitable for human settlement and cultivation, which restrains the vegetation recovery. The marginal increase of NDVI rate is increasing with elevation and maintain steady within the 600-900 m, however, it decreases when the elevation is above 900 m. The inconsistent changes due to the regions with high elevation are mainly underlain by limestone in the study area, differential dissolution in limestone prone to form steep terrain provides kinetic energy for overland flow, which enhances soil erosion under heavy rainfall (Wang et al., 2004b). These conditions are not conducive to the vegetation restoration in these regions.

4.4. Effects of ecological restoration projects on vegetation growth

It is well recognized that climate change and human activities are two primary drivers of vegetation growth. Implementation of ecological restoration projects in karst regions was considered to be one of the major human activities contributing to vegetation growth (Tong et al., 2017; Brandt et al., 2018). We divided the time period into two subperiods based on the time of initiation of karst rocky desertification control projects, namely, pre-2008 and post-2008. The percentage of the area from downtrend to uptrend of NDVI is larger in karst regions (8.9%) than in non-karst region (6.3%) (Fig. 9a). Urban-rural area showed a larger percentage of the area from downtrend to uptrend after 2008 (Fig. 9b). This results are consistent with the aim of karst rocky desertification restoration projects, indicating ecological projects contribute to vegetation greening in the study area. Similar phenomena were reported in Guizhou and Guangxi provinces of China (Tong et al., 2016; Tian et al., 2017), where the area of rocky desertification reduced 19.0% and 8.8% from 2005 to 2011, respectively (National Bureau of Statistics of China. http://www.stats.gov.cn/).

4.5. Implications and research limitations

Chinese central and local governments have made great efforts to restore ecological environment in the karst regions. Our study revealed that the largest rate in vegetation growth occurred in the area within 500–900 m, implying that this region can be the preferred afforestation habitat for vegetation restoration in the future. On the other hand, the lowest NDVI increase rate was observed in the region dominated by limestone areas above 900 m, therefore, special attention should be paid to this region to prevent vegetation degradation. Meanwhile, several reports have shown that revegetation will consume soil water and led to local water shortages (Schwärzel et al., 2019; Škerlep et al., 2020). Many scientists have indicated that trees in the karst regions have complex water resource utilization structures (Zhou et al., 2018; Peng et al., 2019a, 2019b), therefore, the karst-related characteristics of water storage could be utilized efficiently for vegetation growth to cope with water consumption. For example, forest trees have deep roots and are suitable for planting in the karst regions with fissures to exploit deep water. In addition, due to rapid water infiltration into the deep subsurface in karst regions, berms and earth dams could be used to keep water and to raise the water level in creeks for irrigation, providing sufficient soil moisture for vegetation regrowth. In addition to restoration and reconstruction projects, the economic development and policy are the driving forces of vegetation growth. For instance, changes in land use resulting from urbanization and the management model of agriculture are important factors affecting the vegetation cover change

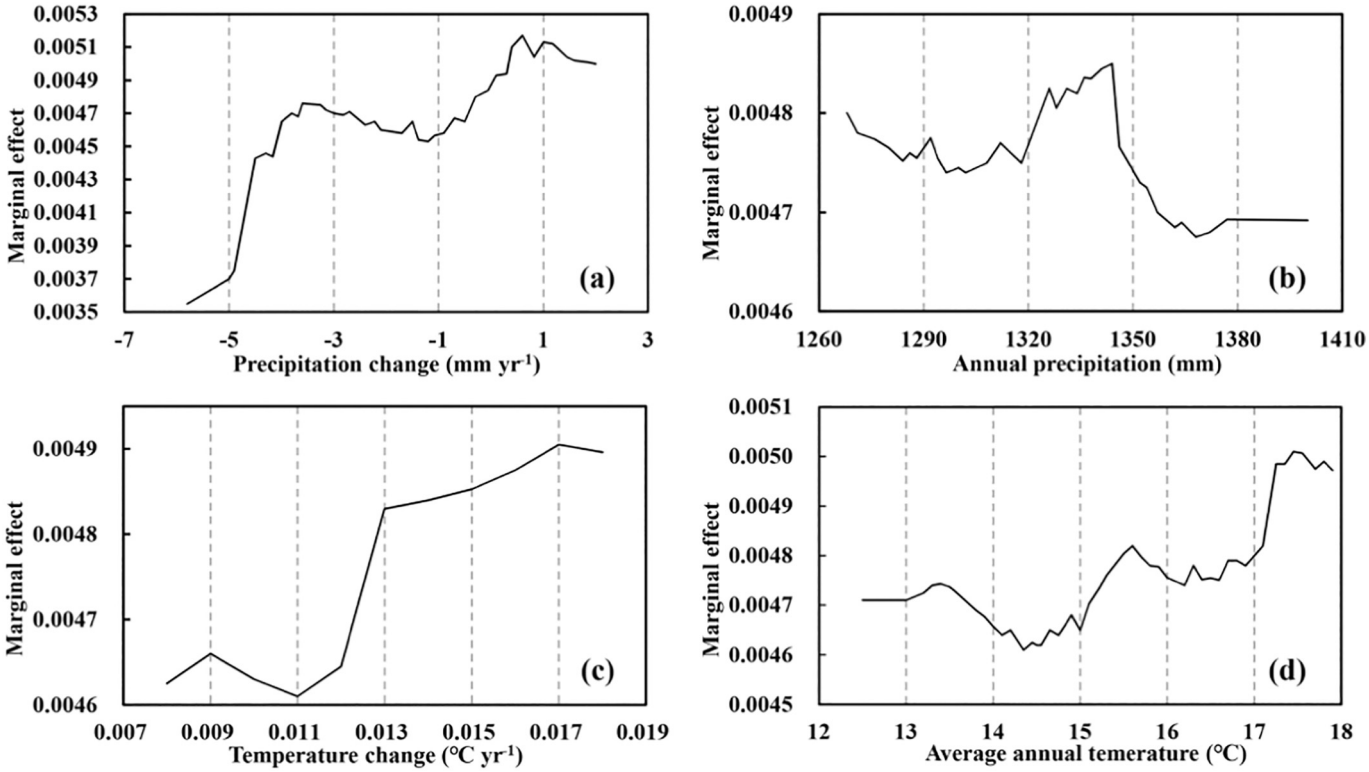

Fig. 7. Marginal effect of climate factors on temporal change in NDVI.

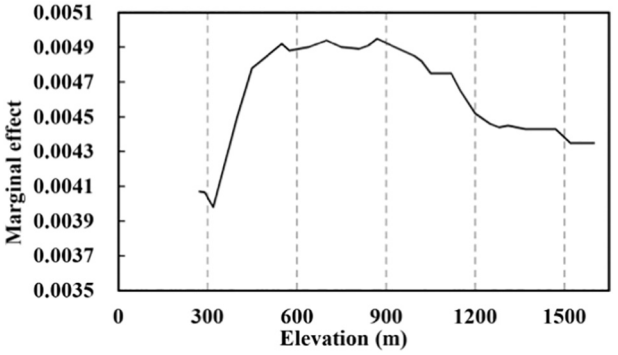

Fig. 8. Marginal effect of elevation on temporal change in NDVI.

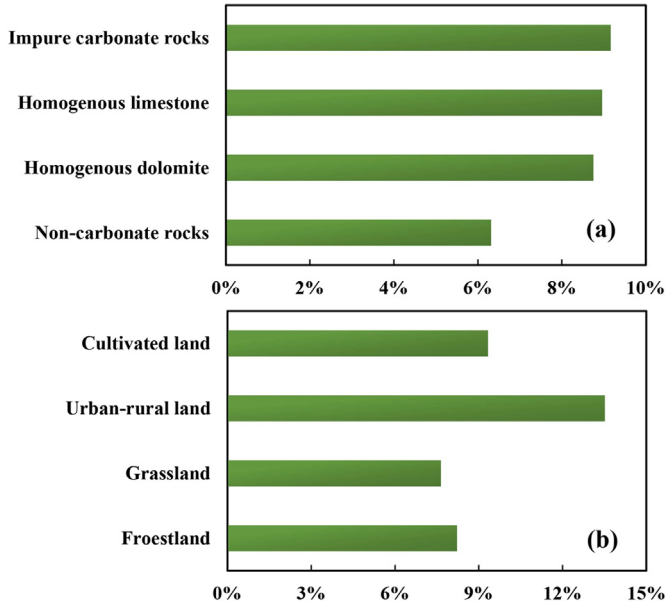

Fig. 9. Proportion of vegetation cover trend from downtrend to uptrend before and after 2008 in each lithology (a) and land-use type (b).

(Geest et al., 2010). In order to increase income, large numbers of labor forces going out for work, migration changes the structure of the original population and influences regional land use and vegetation growth. However, because of the limitations of available social and economic census data, these anthropogenic activities were not taken into account in our study. Thus, more work is needed to quantitatively analyze the relationship between the vegetation cover change and various human factors.

5. Conclusions

In this study, we analysis the spatial-temporal patterns and identify driving factors for vegetation cover change in a typical karst trough valley of southwest China from 2000 to 2016. Our results revealed that an increasing trend in vegetation cover was occurred in most areas (71.44%), and the vegetation cover trends are rather persistent in the karst trough valley. There was a significant heterogeneity in the vegetation cover change and persistent. Precipitation change was the dominant factor affecting vegetation cover change, and wetting promotes vegetation growth. Vegetation growth is slow where limestone dominates, while vegetation is prone to recovery in the region between 500 and 900 m in elevation. Karst vegetation restoration projects should pay attention to the limestone regions above 900 m in elevation in the study area. The quantified information confirms the need to take the lithology into consideration for designing effective ecological recovery projects. The findings could provide a point of reference for identifying drivers on vegetation cover change.

Declaration of Competing Interest

The authors declare that they have no known competing financial interests or personal relationships that could have appeared to influence the work reported in this paper.

Acknowledgments

This study was supported by the National Key Research and Developmental Program of China (2016YFC0502306), the Graduate Scientific Research and Innovation Foundation of Chongqing (CYB18073), the Fundamental Research Funds for the Central Universities (XDJK2020C013) and Chongqing Municipal Science and Technology Commission Fellowship (cstc2018jcyj-yszx0013).

References

Basak, S., Kar, S., Saha, S., et al., 2019. Predicting the direction of stock market prices using tree-based classifiers. N. Am. J. Econ. Financ. 47, 552–567.
Brandt, M., Yue, Y., Wigneron, J.P., et al., 2018. Satellite - Observed Major Greening and Biomass increase in South China Karst during recent Decade. Earth's Future 6, 1017–1028.
Breiman, L., 2001. Random For. Mach. Learn. 45, 5–32.
Cai, H., Yang, X., Wang, K., et al., 2014. Is forest restoration in the Southwest China karst promoted mainly by climate change or human-induced Factors? Remote Sens. 6, 9895–9910.
Cao, J., Yan, D., Zhang, C., et al., 2004. Karst ecosystem constrained by geological conditions in Southwest China. Earth Environ. 32, 1–8 (in Chinese).
Chang, Q., Zhang, J., Jiao, W., et al., 2016. A Comparative Analysis of the NDVIg and NDVI3g in monitoring Vegetation Phenology changes in the Northern Hemisphere. Geocarto Int. 33, 1–20.
Chatzis, S.P., Siakoulis, V., Petropoulos, A., et al., 2018. Forecasting stock market crisis events using deep and statistical machine learning techniques. Expert Syst. Appl. 112, 353–371.
Chen, C., Park, T., Wang, X., et al., 2019. China and India lead in greening of the world through land-use management. Nat. Sustain. 2, 122–129.
Fensholt, R., Langanke, T., Rasmussen, K., et al., 2012. Greenness in semi-arid areas across the globe 1981–2007 — an Earth observing Satellite based analysis of trends and drivers. Remote Sens. Environ. 121, 144–158.
Fukuda, S., Yasunaga, E., Nagle, M., et al., 2014. Modelling the relationship between peel colour and the quality of fresh mango fruit using Random Forests. J. Food Eng. 131, 7–17.
Gang, C., Zhao, W., Zhao, T., et al., 2018. The impacts of land conversion and management measures on the grassland net primary productivity over the Loess Plateau, Northern China. Sci. Total Environ. 645, 827–836.
Gao, Y., Huang, J., Li, S., et al., 2012. Spatial pattern of non-stationarity and scale-dependent relationships between NDVI and climatic factors — a case study in Qinghai-Tibet Plateau, China. Ecol. Indic. 20, 170–176.
Geest, K.V.D., Vrieling, A., Dietz, T., 2010. Migration and environment in Ghana: a cross-district analysis of human mobility and vegetation dynamics. Environ. Urban. 22, 107.
Gunn, S.R., 1998. Support Vector Machines for Classification and Regression. University of Southampton Technical report.
Guo, P., Li, M., Luo, W., et al., 2015. Digital mapping of soil organic matter for rubber plantation at regional scale: an application of random forest plus residuals kriging approach. Geoderma. 237-238, 49–59.
Hou, W., Gao, J., Wu, S., et al., 2015. Interannual Variations in Growing-season NDVI and its Correlation with climate Variables in the Southwestern Karst Region of China. Remote Sens. 7, 11105–11124.
Hurst, H.E., 1951. Long term storage capacity of reservoirs. Trans. Am. Soc. Civ. Eng. 116, 770–808.
Jiang, Z., Lian, Y., Qin, X., 2014. Rocky desertification in Southwest China: Impacts, causes, and restoration. Earth Sci. Rev. 132, 1–12.
Jiang, L., Jiapaer, G., Bao, A., et al., 2017. Vegetation dynamics and responses to climate change and human activities in Central Asia. Sci. Total Environ. 599-600, 967–980.
Kang, C., Zhang, Y., Wang, Z., et al., 2017. The driving force Analysis of NDVI dynamics in the trans-boundary Tumen River Basin between 2000 and 2015. Sustainability. 9, 2350.
Lamchin, M., Lee, W.K., Jeon, S.W., et al., 2017. Long-term trend and correlation between vegetation greenness and climate variables in Asia based on satellite data. Sci. Total Environ. 618, 1089–1095.
Lin, X., Zhang, D., 1999. Inference in generalized additive mixed models by using smoothing splines. J. Royal Statist. Soc. Seri. B. 61, 381–400.
Liu, Y., Li, Y., Li, S., et al., 2015. Spatial and Temporal patterns of Global NDVI Trends: Correlations with climate and Human Factors. Remote Sens. 7, 13233–13250.
Liu, H., Zhang, M., Lin, Z., et al., 2018. Spatial heterogeneity of the relationship between vegetation dynamics and climate change and their driving forces at multiple time scales in Southwest China. Agric. For. Meteorol. 256-257, 10–21.
Mann, H.B., 1945. Nonparametric tests against trend. Econometrica. 13, 245–259.
Pan, T., Zou, X., Liu, Y., et al., 2017. Contributions of climatic and non-climatic drivers to grassland variations on the Tibetan Plateau. Ecol. Eng. 108, 307–317.
Peng, X., Dai, Q., Ding, G., et al., 2019a. The role of soil water retention functions of near-surface fissures with different vegetation types in a rocky desertification area. Plant Soil 441, 587–599.
Peng, W., Kuang, T., Tao, S., 2019b. Quantifying influences of natural factors on vegetation NDVI changes based on geographical detector in Sichuan, western China. J. Clean. Prod. 233, 353–367.
Qi, X., Jia, J., Liu, H., et al., 2019. Relative importance of climate change and human activities for vegetation changes on China's silk road economic belt over multiple timescales. Catena. 180, 224–237.
Qin, C., Lu, Y., Bao, L., et al., 2009. Simple digital terrain analysis software (SimDTA 1.0) and its application in fuzzy classification of slope positions. Geo-Inform. Sci. 11, 737–743 (in Chinese).
Schwärzel, K., Zhang, L., Montanarella, L., et al., 2019. How afforestation affects the water cycle in drylands: a process-based comparative analysis. Glob. Chang. Biol. 26, 944–959.
Sen, P.K., 1968. Estimates of the regression coefficient based on Kendall's tau. Publ. Am. Stat. Assoc. 63, 1379–1389.
Shao, J., Wang, S., Wei, C., 2006. A Conceptual Analysis of Karst Ecosystem Fragility. Prog. Geogr. 25, 1–9.
Škerlep, M., Steiner, E., Axelsson, A., et al., 2020. Afforestation driving long-term surface water browning. Glob. Chang. Biol. 26, 1–10.
Steyrl, D., Scherer, R., Faller, J., et al., 2015. Random forests in non-invasive sensorimotor rhythm brain-computer interfaces: a practical and convenient non-linear classifier. Biomed. Eng. 61, 77–86.
Szilárd, S., László, E., Zoltán, K., et al., 2018. NDVI dynamics as reflected in climatic variables: spatial and temporal trends-a case study of Hungary. GISci. Remote Sensing. 57, 1–26.
Tao, J., Xu, T., Dong, J., et al., 2017. Elevation-dependent effects of climate change on vegetation greenness in the high mountains of Southwest China during 1982-2013. Int. J. Climatol. 38, 2029–2038.
Tian, Y., Bai, X., Wang, S., et al., 2017. Spatial-temporal changes of Vegetation Cover in Guizhou Province, Southern China. Chin. Geogr. Sci. 27, 25–38.
Tong, X., Wang, K., Brandt, M., et al., 2016. Assessing future vegetation trends and restoration prospects in the Karst Regions of Southwest China. Remote Sens. 8, 357.
Tong, X., Wang, K., Yue, Y., et al., 2017. Quantifying the effectiveness of ecological restoration projects on long-term vegetation dynamics in the karst regions of Southwest China. Int. J. Appl. Earth Obs. Geoinf. 54, 105–113.
Tong, X., Brandt, M., Yue, Y., et al., 2019. Increased vegetation growth and carbon stock in China karst via ecological engineering. Nat. Sustain. 1, 44–50.
Tucker, C.J., Slayback, D.A., Pinzon, J.E., et al., 2001. Higher northern latitude normalized difference vegetation index and growing season trends from 1982 to 1999. Int. J. Biometeorol. 45, 184–190.
Wang, S., Ji, H., Ouyang, Z., et al., 1999. Preliminary study on weathering and pedogenesis of carbonate rock. Sci. China Seri. D. 42, 572–581.
Wang, S., Liu, Q., Zhang, D., 2004a. Karst rocky desertification in southwestern China: geomorphology, landuse, impact and rehabilitation. Land Degrad. Dev. 15, 115–121.
Wang, S., Li, L., Sun, X., et al., 2004b. How types of carbonate rock assemblages constrain the distribution of karst rocky decertified land in Guizhou province. In: PR China: Phenomena and Mechanisms. Land Degradation and Development. 15. pp. 123–131.
Wang, K., Zhang, C., Chen, H., et al., 2019. Karst landscapes of China: patterns, ecosystem processes and services. Landsc. Ecol. 34, 2743–2763.
Yuan, D., 1997. Rock desertification in the subtropical karst of South China. Zeitschrift für Geomorphologie N. F. 108, 81–90.
Yuan, D., 2014. The Research and Countermeasures of Major Environmental Geological Problems in Karst Areas of Southwest China. Science Press, Beijing, China.
Zewdie, W., Csaplovics, E., Inostroza, L., 2017. Monitoring ecosystem dynamics in northwestern Ethiopia using NDVI and climate variables to assess long term trends in dryland vegetation variability. Appl. Geogr. 79, 167–178.
Zhang, M., Wang, K., Liu, H., et al., 2018. Effect of ecological engineering projects on ecosystem services in a karst region: a case study of Northwest Guangxi, China. J. Clean. Prod. 183, 831–842.
Zhao, A., Zhang, A., Lu, C., et al., 2017. Spatiotemporal variation of vegetation coverage before and after implementation of grain for Green Program in Loess Plateau, China. Ecol. Eng. 104, 13–22.
Zhou, J., Tang, T., Yang, P., et al., 2012. Inference of creep mechanism in underground soil loss of karst conduits I. Conceptual model. Nat. Hazards 62, 1191–1215.
Zhou, Q., Luo, Y., Zhou, X., et al., 2018. Response of vegetation to water balance conditions at different time scales across the karst area of southwestern China-a remote sensing approach. Sci. Total Environ. 645, 460–470.